Earth and Planetary Science Letters, in press.

Chicxulub impact ejecta from Albion Island, Belize

Kevin O. Pope[a], Adriana C. Ocampo[b], Alfred G. Fischer[c], Walter Alvarez[d], Bruce W. Fouke[e], Clyde L. Webster, Jr.[f], Francisco J. Vega[g], Jan Smit[h], A. Eugene Fritsche[i], and Philippe Claeys[j]

[a]Geo Eco Arc Research, 3220 N Street NW, Suite 132, Washington, DC 20007
Phone/Fax: 202-965-5056 e-mail: kpope@primenet.com

[b]Jet Propulsion Laboratory, California Institute of Technology,
MS 183-601, 4800 Oak Grove Drive, Pasadena, California 91109

[c]Department of Earth Sciences, University of Southern California,
University Park, Los Angeles, California 90089

[d]Department of Geology and Geophysics, University of California, Berkeley,
California 94720

[e]Department of Geology, University of Illinois at Urbana-Champaign, Urbana,
Illinois, 61801

[f]Geoscience Research Institute, Loma Linda University, Loma Linda,
California 92350

[g]Instituto de Geologia, Universidad Nacional Autonoma de Mexico
Ciudad Universitaria, Mexico, D.F.

[h]Institute of Earth Sciences, Vrije Universiteit de Boelelaan 1085,
1081 HV Amsterdam, Netherlands

[i]Department of Geological Sciences, California State University,
Northridge, CA 91330

[j]Museum fur Naturkunde, Institut fur Mineralogie, D-10115 Berlin, Germany

Abstract

Impact ejecta from the Albion Formation are exposed in northern Belize. The ejecta come from the outer portion of the continuous ejecta blanket of the Chicxulub crater, which is located 360 km to the northwest. The basal unit of the Albion Formation is a ~1-m-thick clay and dolomite spheroid bed composed of up to four discrete flows. The clay spheroids are altered impact glass, and the dolomite spheroids are accretionary lapilli. The upper unit is a ~15-m-thick coarse diamictite bed containing altered glass, large accretionary blocks, striated, polished, and impacted cobbles, and rare shocked quartz. The abundance of accretionary clasts, evidence for atmospheric drag sorting, and the presence of multiple flows in the Albion Formation indicate that atmospheres play an important role in the formation of the outer portions of continuous ejecta blankets of large craters.

1. Introduction

The Albion Formation was first described by Ocampo et al. [1] in a quarry on Albion Island located in the Hondo River of northern Belize (Fig. 1). Sedimentologic and petrographic evidence suggest that the Albion Formation is proximal impact ejecta and its stratigraphic position overlying Late Cretaceous platform carbonates indicates that the ejecta most likely come from the Chicxulub impact crater, which lies approximately 360 km northwest of Albion Island [1]. The Albion quarry, together with a series of Albion Formation outcrops we discovered on the Mexican side of the Hondo River in January 1998, are the closest ejecta exposures yet found to the crater and comprise the only known exposures of the Chicxulub continuous ejecta blanket. In this paper we expand upon this earlier work and report new findings from the ongoing research on Albion Island.

2. Barton Creek Formation

The Barton Creek Formation on Albion Island is composed of a tan-colored, 26-m-thick sequence of dolomitized limestone deposited in a shallow-water platform environment (Fig. 1). Petrographic and outcrop analyses indicate interbedding of shallow subtidal and intertidal sediments, some with nodular molds suggesting periodic emergence and evaporite deposition. Cathodoluminescence (CL) petrography indicates a complex paragenetic sequence of calcite cementation and dolomitization [2]. Benthic foraminifera fossils are present in the section, but they are too recrystallized to be identified. A new species of fossil crab, *Carcineretes planetarius* [3] (Fig. 2a), and nerineid gastropods (Fig. 2b) are found near the base of the exposed section (Fig. 1). Flores [4] interpreted the Barton Creek Formation as representing a shallow, back-reef lagoon environment. This is consistent with the gastropods and crabs, as well as with the overall restricted fauna and lithology of the Albion quarry.

The Barton Creek Formation in central Belize contains Upper Cretaceous fossil rudistids, miliolids, rotalids, *Dyciclina* sp., *Lockhartia* sp., *Nummoloculina* sp., and *Valvulina* sp. [4]. The nerineid gastropods from Albion Island have infolding wall structures (Fig. 2b) characteristic of the last

developmental stage, indicating a Campanian to Maastrichtian age. Vega et al. [3] propose a Maastrichtian age for the *Carcineretes planetarius* crabs found at Albion Island. The only other member of *Carcineretes*, *C. woolacotti*, comes from the early Maastrichtian [5]. These findings, together with the $^{87}Sr/^{86}Sr$ isotope ratios (0.70786-0.70796) from Barton Creek Formation reported by Ocampo et al. [1], suggest a Maastrichtian age for the dolomitized limestones underlying the impact ejecta.

The Barton Creek Formation in the quarry was folded into a gently plunging anticline, the apex of which was eroded prior to deposition of the overlying Albion Formation. The upper surface of the Barton Creek Formation is irregular with local abrupt relief of 20-50 cm and preserved patches of caliche (Fig. 3). This caliche is composed of poorly sorted, angular fragments of the Barton Creek Formation dolomite re-cemented with micritic dolomite and coarse-grained calcite with iron oxide crusts. Such a surface is similar to the caliche caps found on emergent portions of the Pleistocene Yucatan platform [6]. These findings indicate that Albion Island was emergent prior to the deposition of the Albion Formation.

3. Albion Formation spheroid bed

The spheroid bed ranges in thickness from 0.10-1.72 m, but most exposures are ~1 m thick. The basal, and occasionally the upper, contact is a ~2-cm-thick brown clay layer (Fig. 4) with pronounced slickensides. Similar clay layers occur along shear planes that cut diagonally across the bed (Fig. 5). Typically, the upper contact is marked by the abrupt appearance of cobbles of the overlying diamictite bed, but with little change in the matrix (Fig. 5). Four distinct strata with gradational contacts are differentiated by clast type and foliation (Fig. 1). All four strata contain 10-30% (by volume) dolomite spheroids, 1-10 mm in diameter. They also contain 10% (by volume) flakes and angular clasts of brown clay, 1-3 mm in diameter. Spheroids are supported in a weakly consolidated, fine-grained, dolomite and clay matrix. Rare dolomite spheroids reach sizes of 20-30 mm. Green clay spheroids 1-10 mm in diameter comprise 10-30% (by volume) of stratum 1 and grade upward into the base of stratum 2 (2a, Fig 1). Most spheroids fall in the 5-10 mm size range. No size grading of spheroids is apparent in outcrop.

Stratum 1 is 15-20 cm thick. The dolomite and green clay spheroids are flattened (Fig. 6) and deposited with the long axis parallel to the underlying Barton Creek Formation surface (imbricated), giving the bed a foliated appearance, which follows the microtopography. Stratum 2 is 25-40 cm thick, contains slightly flattened dolomite spheroids, and has faint foliation. Stratum 3 is 40-50 cm thick and contains spherical to slightly oblate dolomite spheroids, distinct foliation, and 10% (by volume) white, chalky, angular dolomite clasts in the same size distribution as the spheroids. Stratum 4 is 40-50 cm thick and has the same composition as stratum 3, but no foliation.

3.1. Matrix and dolomite spheroids

The matrix of the spheroid bed is composed of sucrosic 25-50 μm dolomite crystals with concentric red/yellow CL zonations, which contrast with the bright, concentric red/orange CL zonations in the dolomite crystals of the spheroids [2]. The matrix and spheroids contain interstitial iron oxide and smectite. The smaller (<5 mm) dolomite spheroids are composed of crystals of uniform size (~25 μm). Most dolomite spheroids in the 10-25 mm range have

concentric bands of fine and coarse crystals and iron oxide staining surrounding an angular core (Fig. 7) Coarse spheroid bands have crystal sizes up to 500 μm, but most bands have 50-75 μm crystals. Many of the larger crystals within these bands have black opaque cores (Fig. 7c). One large dolomite spheroid contains a core composed of two smaller spheroids joined together (Fig. 8). The angular cores are composed of a white, chalky, fine-grained (~10 μm) dolomite (Fig. 7a) that is similar to the dolomite clasts in the upper strata of the spheroid bed.

3.2. Clay spheroids

The green clay spheroids at the base of the spheroid bed have a dull, waxy appearance. X-ray diffraction (XRD) analyses indicate they are mostly smectite. Petrographic and microprobe analyses reveal that portions of some spherules are isotropic and have Si/Al ratios (Table 1) higher than typical smectites, as found in other K/T boundary clay spherules [7, 8]. Microprobe analyses of major oxides indicate that the green clay spheroids are compositionally similar to the Haitian palagonites formed from K/T boundary glass spherules (Table 1). The typical size (mostly 5-10 mm in diameter) of the Albion Formation spheroids is larger than that of the Haitian spherules (mostly <2 mm in diameter [7, 9]). Scanning electron micrographs (SEM) and thin sections of the clay spheroids show vesicular and spherulitic textures typical of devitrified glass (Fig. 9).

4. Albion Formation diamictite bed

Ocampo et al. [1] estimated the maximum thickness of the diamictite to be about 15 m, but an erosion surface cuts the top and its original thickness is unknown. The diamictite is weakly consolidated, unstratified, poorly sorted, and is composed mostly of matrix supported carbonate and clay clasts. Carbonate clasts are angular to subrounded and range in size from sub-millimeter grains to boulders about 8 m in diameter.

4.1. Carbonate clasts and matrix

Due to the abundance of large clasts in the diamictite, we employed a grain size analysis technique using the cross-sectional area of clasts, similar to that used in thin section analysis. We measured clasts diameters within 1 m by 1 m grids at four outcrops in the quarry, and in photographs of a 66-m-long freshly cut face of the quarry. The outcrops were randomly chosen from the base (saddle and cut 1 lower part) and upper (cut 1 upper part, cut 2) portions of the diamictite bed. We measured all clasts larger than 0.8 cm within the grids and larger than 2 m in the photographs (smaller clasts were not detected in the photographs). The percent matrix (defined here as clasts smaller than 0.8 cm in diameter) was calculated for each grid. The results of these analyses are shown in a series of histograms for the grid data (Fig. 10) and as a graph of the cumulative percentage (area) for the combined grid and photograph-based data (Fig. 11). Assuming uniform density of materials, these data are good proxies for weight percentages more commonly used in such analyses. These figures illustrate the poorly sorted nature and heterogeneity of the diamictite bed.

Most of the carbonate clasts are dolomitized limestone and the nonclastic component of the matrix is a micritic dolomite (10-60 μm crystals) with minor amounts of interstitial clay and iron oxide. Multiple generations of CL-distinct dolomite cements are found in the matrix and in the carbonate clasts [2]. The diamictite bed contains rare concentric dolomite spheroids

10-20 mm in diameter and a few large blocks (up to 4.5 m in diameter) with lithic cores and 7-75 cm-thick rinds of material similar in texture and composition to the diamictite matrix (Fig. 12). Rare carbonate clasts exhibit striations in a single or occasionally multiple directions and in many cases terminate in an abrupt angular surface (Fig. 13a). These striations range from microscopic sets that grade into a fine polish, to parallel grooves 1-2 mm deep. Sand-sized carbonate grains occur within some striae. In one sample, a dark dolomite rock chip penetrated the clast to form a pit with a striated wall (Fig. 13b). Ocampo et al. [1] reported finding a clay pocket filled with radially fibrous calcite spherules that they called pisoids. We found another similar pocket in 1995. These new radially fibrous calcite spherules included many with angular cores of a dark gray dolomite. The calcite spherules have etched surfaces and wart like protrusions (Fig. 14) similar to the smaller altered glass spherules from the K/T boundary [9].

4.2. Clay clasts and other components

Green clay clasts comprise about 10% (by weight) of the diamictite bed. They range in size from <1 mm to 40 mm, but most are <10 mm in diameter. Petrographic, XRD, SEM, and microprobe analyses of the clays reveal they are smectite and palagonite. Compositionally these palagonites are similar to those of the spheroid bed, except that they contain slightly more K and Fe (Table 1). Many of the clay fragments have the same vesicular textures and spherulitic devitrification features found in the green clay spheroids of the spheroid bed (Fig. 15).

Authigenic quartz found within vugs in the diamictite bed contains anhydrite inclusions. Acid leach residues from the diamictite contain common gypsum as finely disseminated crystals. Apparently sulfates have been mostly leached from the deposits. We found a single detrital quartz grain in the acid leach residues that has one prominent set and a second clear set of planar deformation features (Fig. 16), indicative of shock. Detrital quartz grains were extremely rare in the over 1 kg of diamictite that was processed and only one shocked quartz grain was found.

5. Interpretations

The shocked quartz and impact-penetrated cobbles add to evidence provided by Ocampo et al. [1] that the Albion Formation is of impact origin. The penetrating rock chip must have impacted under pressures and/or temperatures sufficient to plastically deform carbonates [10], since impacts between solid particles produce radial fractures and spallation zones [11], not the grooved penetrating features we observed. The origin of this high temperature/pressure environment is uncertain, but may have developed during particle ejection from the crater or within the ejecta curtain. The impact-penetrating chip is part of a cluster of pits and striations that radiate away from the tip of the pointed cobble in parallel sets (Fig. 13). This suggests that the cobble was rotating as it past through (in a relative sense) a cloud of finer debris. Similar features are found in other ejecta [12] and these surface features are common on pebbles and cobbles in the Chicxulub ejecta deposits in central Belize [13]. Indications that the Barton Creek Formation underlying the Albion Formation is probably Maastrichtian, provides an improved temporal link between the Albion Formation and the nearby K/T Chicxulub crater.

The Barton Creek Formation carbonates are composed of several size-distinct and CL-distinct generations of

cement and replacement dolomite, which are different with respect to size and CL from the dolomites in either the spheroid or the diamictite beds. Furthermore, the dolomites in the spheroid bed are different in size, CL character, and composition from the dolomites comprising the matrix and allochthonous blocks of the diamictite bed. No evidence of dolomite cement overgrowths on detrital dolomite crystals or fragments was observed with [illegible] in either the spheroid or the diamictite beds. These observations suggest that: 1) the fluids that dolomitized the Barton Creek Formation, spheroid bed, and diamictite bed were chemically distinct from one another; 2) the Barton Creek Formation limestone was dolomitized prior to deposition of the ejecta; and 3) neither the spheroid bed dolomites nor most of the dolomitized allochthonous blocks in the diamictite bed were derived from the directly underlying Barton Creek Formation.

Figure 11 indicates that the diamictite contains two populations of clasts. The grid data represent one normally distributed population with a modal size (excluding matrix) of -5 to -6 phi (3.2-6.4 cm, Fig. 10), which plots close to a straight line on the probability scale of the cumulative % curve (Fig. 11). The photographic data, representing the larger clast sizes (-11 to -13 phi, ~ 2-8 m), do not plot close to the straight line of the grid data. Such a deviation from a single straight line is a good indication that two populations are involved [14]. While it is possible that the different measurement techniques have some effect on the results, we note that the proposed difference between the two populations is that large clasts are too abundant to be the tail of a single population distribution. One would expect if the photographic technique did introduce some error, it would underestimated the number of large clasts. The lack of clasts in the -8 to -11 phi size range (~25 200 cm) may in part be an artifact of the sampling, since it is difficult to detect clasts in this range in the photographs. Nevertheless, we emphasize that no clasts in this size range were found in the randomly placed grids. Furthermore, we note that clasts this size were very rarely encountered during the field work and there may be a true gap in clast size between the two proposed populations.

Ocampo et al. [1] interpreted the green clay spheroids and clasts to be altered impact glass and our additional analyses support this. The microprobe analyses indicate that no glass is preserved, but much of the clay is palagonite, a common alteration product of glass. The carbonate spheroids found in the spheroid bed and rarely in the diamictite bed are interpreted to be accretionary lapilli, which are commonly found in pyroclastic deposits. Ocampo et al. [1] proposed an accretionary lapilli origin for the spheroids with cores, but suggested other possible origins for the spheroids without cores. Pyroclastic deposits commonly contain lapilli with and without cores [15] and our petrographic examination of the carbonate spheroids found no significant differences in the matrix composition between spheroids with and without cores. The radially fibrous calcite spherules found in the diamictite bed may be another form of accretionary lapilli, given that many of these also have lithic cores. Their fibrous crystalline structure and tektite-like surfaces noted above indicate that these spherules may have crystallized from calcite melt.

The complex stratification within the spheroid bed indicates that the composition of the volatile-rich plume that accreted the lapilli was rapidly evolving as it reached the southern end of the Yucatan Peninsula. The several discrete, thin strata suggest multiple flows with different amounts of glass, lapilli, and carbonate clasts were involved. The

absence of graded beds and the common lack of shear zones between strata within the spheroid bed suggest that the debris may have been in part deposited by turbulent flows. Pyroclastic air fall deposits are usually normally graded and laminar flows produce inverse grading due to the expulsion of large clasts from the base by shear forces [16]. Nevertheless, the foliation (imbrication) found in the spheroid bed is commonly observed in pyroclastic flows, where it is attributed to shear during laminar flow [17]. We also note that a few spheroid bed exposures have shear planes (Fig. 4 and 5). The presence of foliation and basal shear in some strata, and the lack of these features in others, may indicate that the flows that deposited the spheroid bed were changing between turbulent and laminar. Changes from a turbulent to laminar flow regime are typical of pyroclastic flows where the loss of volatiles (deflation) reduces buoyancy forces [16]. Such flow regime changes are typical of distal pyroclastic flows shortly before deflation and friction halt the flow [18]. This is consistent with our geological reconnaissance, which indicates Albion Island is near the terminus of the continuous ejecta blanket.

We interpret the large blocks with coatings of matrix material in the diamictite bed as accretionary blocks similar in origin to the carbonate spheroids. Ocampo et al. [1] originally described one of these large (3 m) clasts from Albion Island as a mud-coated boulder (Fig. 11 in [1]). They suggested that the mud coating may be genetically related to a large mudball also found in the diamictite bed (Fig. 14 in [1]), which was interpreted as being similar in origin to mudballs in terrestrial debris flows. In 1998 a better exposure (due to erosion) of this mudball revealed that it is a giant mud-coated boulder (Fig.12), not a mudball. Mudballs form in debris flows when fine-grained sediment (mud) is ripped up and carried along in the flow [19]. In contrast, mud-coated boulders like those found on Albion Island have not been reported from debris flows. We now recognize that these large mud-coated boulders are similar in structure and composition to the accretionary lapilli, hence our interpretation of them as accretionary blocks. These large accretionary blocks indicate that the diamictite bed is also derived from debris once suspended in a volatile-rich plume, but one with large clasts and sufficient energy to transport 4.5-m-diameter boulders.

6. Comparisons with other ejecta deposits

Surface exposures of proximal ejecta from large impact craters are rare on Earth. Prior to the Belize discoveries, the best-known examples were from the Ries crater in Germany [20, 21] and the Sudbury crater in Canada (e.g. the Onaping Formation, [22]). The Alamo breccia in Nevada [23] is probably proximal ejecta from a large impact, but no crater has been identified. The Pelarda Formation in Spain may also be proximal impact ejecta from the Azuara structure [24, 25], but the impact origin of this material is controversial. Ries (~24 km diameter) is much smaller than Chicxulub. The exposures of Ries ejecta extend about two crater radii (24 km) from the center of the crater, whereas Albion Island is over three crater radii (360 km) from the center of the Chicxulub. Thus, Albion Island represents a more distal environment in both relative and absolute terms. Given these contrasts in size and proximity, depositional processes may have been different for the Ries and Albion Island deposits. Sudbury (~200 km) is approximately the same size as Chicxulub, but no ejecta from outside the crater is preserved. Ejecta from other large craters is either poorly preserved (e.g. Popagai crater) or is known only from drilling (e.g., Chesapeake Bay crater). The

Albion Formation is the only known well-exposed example of the continuous ejecta blanket from a large (>50 km diameter) crater. Chicxulub ejecta from farther south in Belize [10] are probably not part of the continuous ejecta blanket.

There are no good impact analogues to the Albion Formation spheroid bed. The best analogy is a volcanic pyroclastic flow, however we know of no volcanic examples of carbonate accretionary lapilli or blocks. Carbonate accretionary lapilli are reported from the Alamo breccia [26] and from Azuara [25]. They are also found in more distal Chicxulub ejecta in Mexico [27, 28]. Silicate accretionary lapilli are present in crater fill breccias of the Sudbury [22] and Manson [29] craters. The melt-rich ejecta called suevite at Ries crater contain silicate spherules, chondrules, and accretionary lapilli [30]. In none of these examples do lapilli form a distinct stratum beneath coarser ejecta, and in fact, the stratigraphy at Ries crater appears reversed, where the lapilli-bearing strata of the suevite overlie the coarse Bunte breccia.

The Bunte breccia of the Ries crater and the Bunte-like breccia drilled on the Chicxulub rim [31] share several characteristics with the Albion Formation diamictite bed [1]. It is important to note, however, that the Bunte breccia at Ries contains no altered glass or accretionary clasts. The Albion Formation diamictite bed contains abundant altered glass and accretionary clasts, and thus appears to be a mixture of Bunte breccia and suevite-like components. The diamictite bed also shares many characteristic with the Onaping Formation of the Sudbury crater [22], notably common altered glass fragments and accretionary lapilli and blocks. We also note close similarities between the clay pockets with radially fibrous calcite spherules in the diamictite bed and some of the "spherulitic dikes" (those that are irregularly shaped bodies not dikes) found in the Onaping Formation, which contain cm-sized spherules with radiating feldspar crystals [22].

7. Continuous ejecta blanket deposition

The widely accepted model for emplacement of the Bunte breccia at Ries crater is ballistic sedimentation [32], where impacting ejecta blocks scour the surface and produce a surface flow composed of minor amounts of ejecta and much local rock. The principal evidence for this model is the abundance of local rock in the Bunte Breccia [21]. Most of the lithologies in the Albion Formation are similar to those of the local Barton Creek Formation and could be the product of scouring by secondary impacts on the Yucatan platform. Nevertheless, this argument is not conclusive, since the upper 2 km of target rock at Chicxulub is also composed of carbonates similar to the Barton Creek Formation [33]. Impact models [34] predict that the high ejection velocities needed to reach Belize would only occur at shallow target depths, or close to the impact center where the deeper crystalline rocks would have been melted (origin of the Albion Formation altered glass). Therefore we cannot rule out the possibility that most of the Albion Formation is composed of primary ejecta from Chicxulub. We note that the more distal ejecta from Ries are also dominated by the uppermost target lithologies [21].

The fact that there is no evidence for major scouring at the base of the Albion Formation, and that the CL studies indicate the diamictite bed and Barton Creek Formation dolomites are different, argues against production by local secondary impacts. Nevertheless, the ejecta may have been produced by such impacts farther up range. More importantly, ballistic

sedimentation does not account for the abundance of accretionary lapilli and blocks in the Albion Formation.

Another model of continuous ejecta blanket emplacement is the ring vortex model [35, 36, 37]. In this model a turbulent cloud of primary ejecta is produced by atmospheric drag induced ring vortices that develop upon breakdown of the advancing ejecta curtain. The turbulent cloud thus produced contains much of the finer ejecta, which is stripped from the ejecta curtain. This model provides a better explanation of the Albion Formation, given the abundance of fine matrix and accretionary and rounded clasts (abrasion in the ring vortices?). The large accretionary blocks in the Albion Formation may attest to the power of this turbulence, which likely reached supersonic speeds [35, 36]. The apparent sorting reflected in the two populations of clasts in the diamictite bed may also be a product of ejecta interaction with the atmosphere. The ring vortex model [36] predicts sorting of clasts in the same size range as that found in Belize.

The complex stratigraphy of the Albion Formation indicates that the ejecta were emplaced by multiple flows of different composition and possibly origin. The origin of the spheroid bed debris may be either jetting or vapor plume entrainment of fine material from the ejecta curtain. The diamictite bed is probably derived from collapse of the main ejecta curtain. These flows may be the product of the complex emplacement processes proposed for fluidized ejecta blankets on Mars and Venus [35, 37].

We propose that ballistic sedimentation on planets with atmospheres may dominate only near the crater rim (perhaps within a final crater radii of the rim), where the initial blast of the vapor plume and the advancing ejecta curtain largely displace the atmosphere, and where permeability in the ejecta curtain has not yet developed. At greater distances, the effects of the atmosphere become significant, secondary impacts are reduced, and ejecta deposition is dominated by material derived from turbulent clouds of debris. This study demonstrates that atmospheres can play an important role in the formation of continuous ejecta blankets of large craters.

8. Acknowledgments

This work was funded by the Exobiology Program of the National Aeronautics and Space Administration and by The Planetary Society. We thank The Planetary Society volunteers and the Albion Stone Company for their help with the fieldwork, and the Belize Geology and Petroleum Office for their permission to conduct the research.

9. References

[1] A.C. Ocampo, K.O. Pope, and A.G. Fischer, Ejecta blanket deposits of the Chicxulub crater from Albion Island, Belize, in: The Cretaceous-Tertiary Event and Other Catastrophes in Earth History, G. Ryder, D. Fastovsky, and S. Gartner, S., eds., Geological Society of America Special Paper 307, p. 75-88, Boulder, Colorado, 1996.

[2] B.W. Fouke, W. Alvarez, Ph. Claeys, A. Ocampo, K.O. Pope, J. Smit, and F.J. Vega, Cathodoluminesence study of carbonate growth phases in bedrock and KT ejecta from the Chicxulub Impact, at the Albion Island quarry, Belize, Geological Society of America Abstracts with Programs, v. 28, p. A-183, 1996.

[3] F.J. Vega, R.M. Feldman, A.C. Ocampo, K.O. Pope, A new species of Late Cretaceous carcineretid crab

(Brachyura: Carcineretidae) from Albion Island, Belize, Journal of Paleontology, 71, 615-620, 1997.

[4] G. Flores, Geology of northern British Honduras: American Association of Petroleum Geologists Bulletin 36, 404-409, 1952.

[5] S.F. Morris, The fossil arthropods of Jamaica, in: Biostratigraphy of Jamaica, E.M. Wright and E. Robinson, eds., Geological Society of America Memoir 182, p. 115-124, Boulder, Colorado, 1993.

[6] W.C. Ward, Quaternary geology of northeastern Yucatan Peninsula, in: Geology and Hydrogeology of the Yucatan and Quaternary Geology of Northeastern Yucatan Peninsula, W.C. Ward, A.E. Weidie, and W. Back, eds., New Orleans Geological Society Publication, p. 23-95, 1985.

[7] B.F. Bohor, and B.P. Glass, Origin and diagenesis of K/T impact spherules - From Haiti to Wyoming and beyond, Meteoritics 30, 182-198, 1995.

[8] D.A. Kring, and W.V. Boynton, Altered spherules of impact melt and associated relic glass from the K/T boundary sediments in Haiti, Geochimica et Cosmochemica Acta 55, 1737-1742, 1991.

[9] G.A. Izett, Tektites in Cretaceous/Tertiary boundary rocks on Haiti and their bearing on the Alvarez impact extinction hypothesis, Journal of Geophysical Research 96, 20,879-20,905, 1991.

[10] J.R Marshall, C. Bratton, K.O. Pope, and A.C. Ocampo, Diagnostic clast-texture criteria for recognition of impact deposits (abstract), Lunar Planetary Science 29, abstract 1134, 1998.

[11] M.S. Prasad, and M. Sudhakar, Collisions in the ejecta plume of the Australasian impact event, Lunar and Planetary Science 27, 1053-1054, 1996.

[12] E.C.T Chao, Mineral produced high pressure striae and clay polish: Key evidence for nonballistic transport of ejecta from Ries crater, Science 194, 615-618, 1976.

[13] A.C. Ocampo, K.O. Pope, and A.G. Fischer, Carbonate ejecta from the Chicxulub crater: Evidence for ablation and particle interaction under high temperatures and pressures (abstract), Lunar Planetary Science 28, abstract 1861, 1997.

[14] G.S. Visher, Grain size distribution and depositional processes, Journal of Sedimentary Petrology 39, 1074-1106, 1969.

[15] R. Schumacher and H.-U. Schmincke, Internal structure and occurrence of accretionary lapilli - a case study at Laacher See Volcano, Bulletin of Volcanology 53, 612-634, 1991.

[16] M.F. Sheridan, Emplacement of pyroclastic flows: A review, in: Ash-Flow Tuffs, C.E. Chapin and W.E. Elston, eds., Geological Society of America Special Paper 180, p. 125-136, Boulder, Colorado, 1979.

[17] C.E. Chapin and G.R. Lowell, Primary and secondary flow structures in ash-flow tuffs of the Gribbles Run paleovalley, central Colorado, in: Ash-Flow Tuffs, C.E. Chapin and W.E. Elston, eds., Geological Society of America Special Paper 180, p. 137-154, Boulder, Colorado, 1979.

[18] K.H. Wohletz and M.F. Sheridan, A model of pyroclastic surge, in: Ash-Flow Tuffs, C.E. Chapin and W.E. Elston, eds., Geological Society of America Special Paper 180, p. 177-194, Boulder, Colorado, 1979.

[19] Bull, W.B., Alluvial fans and near-surface subsidence in western Fresno County, California, U.S. Geological Survey Professional Paper 437-A, 70 p., 1964.

[20] E.C.T. Chao, R. Huttner, and H. Schmidt-Kaler, Principal Exposures of the Ries Meteorite Crater in Southern Germany, 84 p., Bayerisches Geologisches Landesamt, Munchen, 1978.

[21] F. Horz, R. Ostertag, and D.A. Rainey, Bunte Breccia of the Ries: Continuous deposits of large impact craters, Reviews of Geophysics and Space Physics 21, 1667-725, 1983.

[22] T.L. Muir, and W.V. Peredery, The Onaping Formation, in: The Geology and Ore Deposits of the Sudbury Structure, E.G. Pye, A.J. Naldrett, and P.E. Giblin, eds., p. 139-204, 1984.

[23] J.E. Warme, and C.A. Sandberg, Alamo Megabreccia: Record of a Late Devonian impact in southern Nevada: GSA Today 6, 1-7, 1996.

[24] K. Ernston and F. Claudin, Pelarda Formation (Eastern Iberian Chains, NE Spain): Ejecta of the Azuara impact structure, N. Jb. Geol. Palaont. Mh., H10, 581-599, 1990.

[25] K. Ernston and J. Fiebag, The Azuara impact structure (Spain): new insights from geophysical and geological investigations, Geologische Rundschau 81, 403-427, 1992.

[26] J.E. Warme and H.-C. Kuehner, Accretionary carbonate impact-ejecta spherules in the Upper Devonian Alamo Breccia, south-central, Nevada (abstract), Geological Society of America Abstracts with Programs 29, A-80, 1997.

[27] J.M. Grajales N., D.J. Moran, P. Padilla, M.A. Sanchez, E. Cedillo, and W. Alvarez, The Loma Tristes Breccia: A K/T impact-related breccia from southern Mexico (abstract), Geological Society of America Abstracts with Programs, 28, A-183, 1996.

[28] J. Smit, Th.B. Roep, W. Alvarez, A. Montanari, Ph. Claeys, J.M. Grajalez-Nishimura, and J. Bermudez, Coarse-grained, clastic sandstone complex at the K/T boundary around the Gulf of Mexico: Deposition by tsunami waves induced by the Chicxulub impact?, in: The Cretaceous-Tertiary Event and Other Catastrophes in Earth History, G. Ryder, D. Fastovsky, and S. Gartner, S., eds., Geological Society of America Special Paper 307, p. 151-182, Boulder, Colorado, 1996.

[29] B.J. Witzke, and R.R. Anderson, Sedimentary-clast breccias of the Manson impact structure, in: The Manson Impact Structure, C. Koeberl and R.R. Anderson, eds., Geological Society of America Special Paper 302, p. 115-144, Boulder, Colorado, 1996.

[30] G. Graup, Terrestrial chondrules, glass spherules and accretionary lapilli from the suevite, Ries crater, Germany, Earth and Planetary Science Letters 45, 407-418, 1981.

[31] Sharpton, V. L., Marin, L. E., Carney, J. L., Lee, S., Ryder, G., Schuraytz, B. C., Sikora, P., and Spudis, P. D., 1996, A model of the Chicxulub impact basin based on evaluation of geophysical data, well logs, and drill core samples, in The Cretaceous-Tertiary Event and Other Catastrophes in Earth History, edited by G. Ryder, D. Fastovsky, and S. Gartner, Boulder, Colorado, Geological Society of America

Special Paper, v. 307, p. 55-74.

[32] V.R. Oberbeck, The role of ballistic erosion and sedimentation in lunar stratigraphy, Geophysics and Space Physics 13, 337-362, 1975.

[33] W.C. Ward, G. Keller, W. Stinnesbeck, and T. Adatte, Yucatan subsurface stratigraphy: Implications and constraints for the Chicxulub impact, Geology 23, 873-876, 1995.

[34] H.J. Melosh, Impact cratering: A Geologic Process, 245 p, Oxford University Press, New York, 1989.

[35] P.H. Schultz, Atmospheric effects on ejecta emplacement, Journal of Geophysical Research 97, 11,623-11,662, 1992.

[36] O.S. Barnouin-Jha and P.H. Schultz, Ejecta entrainment by impact-generated ring vortices: Theory and experiments, Journal of Geophysical Research 101, 21,099-21,115, 1996.

[37] O.S. Barnouin-Jha and P.H. Schultz, Lobateness of impact ejecta deposits from atmospheric interactions, Journal of Geophysical Research 103, 25,739-25,756, 1998.

FIGURE CAPTIONS

Fig. 1. Stratigraphy of the Albion Island quarry, Belize. Spheroid bed section is from the saddle location; strata 1-4 are described in text, substrata (e.g. 2a, 2b) are subdivisions not found in every quarry location. Clasts in Diamictite bed are schematic. Key to Barton Creek Formation dolomite: a) thick, coarsely crystalline beds with vugs indicative of leached anhydrite nodules, b) thin, finely crystalline beds, c) crossbedded, coarse, calcarenite beds, and d) fine grained, organic-rich, laminated beds with hummocky and ripple crossbedding. Inset: Map with location of Albion Island and the Chicxulub crater.

Fig. 2. Barton Creek Formation: (a) *Carcineretes planetarius* crab (scale bar 10 mm) and (b) nerineid gastropod (scale bar 1 mm). See Fig. 1 for location in section.

Fig 3. Upper contact of the Barton Creek Formation. Note caliche with brecciated surface and dark iron oxide staining. Pen is 14 cm long and rests on land surface at time of impact.

Fig. 4. Albion Island quarry. Near center of photograph is a planar 80-cm-thick Albion Formation spheroid bed exposure with sharp lower (Barton Creek Formation) and upper (Albion Formation diamictite bed) contacts.

Fig. 5. Albion Formation spheroid bed with clay lined shear plane cutting diagonally across the bed near the base. Scale with 10-cm increments rests on Barton Creek Formation contact (total exposure 2 m). Note contact between spheroid bed and diamictite bed at 70 cm, marked by the appearance of cobbles but little change in the matrix.

Fig 6. Dolomite spheroids from the base of the Albion Formation spheroid bed. Note flattened disk shape (scale bar 10 mm).

Fig. 7. Dolomite spheroid (accretionary lapilli) from the Albion Formation spheroid bed: (a) cross-section showing white angular core and concentric bands (scale bar 10 mm); (b) thin section (plain polarized light) showing fine-grained core (dark in transmitted light) with concentric bands of

coarse and fine grain dolomite (scale bar 5 mm); (c) thin section (plain polarized light) of concentric band of coarse crystals showing common, black, opaque cores (scale bar 0.5 mm).

Fig. 8. Thin section (plain polarized light) of dolomite spheroid from the Albion Formation spheroid bed with a core of two highly porous dolomite spheroids (scale bar 10 mm).

Fig. 9. SEM image of a polished section of a palagonite fragment from a spheroid bed green clay spheroid showing a relict vesicle (right) and spherulitic devitrification features (lower left) (scale bar 0.1 mm).

Fig. 10. Histograms of Albion Formation diamictite bed grain size measured in 1 m by 1 m grids from the saddle (SAD), cut 1 lower part (CTL), cut 1 upper part (CTU), and cut 2 (CT2) locations in quarry. Percentages are based on cross-sectional area within the grids. Matrix is all clasts smaller than 0.8 cm. Line on graph depicts mean grain size for the four locations. Phi is a base 2 scale with phi -4 = 0.8-1.6 cm and a phi -8 = 12.8-25.6 cm.

Fig. 11. Albion Formation diamictite bed grain size plotted as cumulative percent (area) on a probability scale. Data in phi -4 to -8 are mean values from grid analysis (Fig. 10). Data for phi -12 and -13 are from analysis of photographs. Note grid data plot near a straight line, indicative of a single normally distributed population.

Fig. 12. Albion Formation diamictite bed accretionary block (diameter 4.5 m); dashed lines demarcate greenish gray core of dolomite and clay surrounded by a 75-cm-thick rind of white dolomite matrix.

Fig. 13. Albion Formation diamictite bed (a) striated dolomite cobble with close-up of upper tip (b) showing penetrating lithic fragment (scale bar in both photographs 10 mm).

Fig 14. Albion Formation diamictite bed calcite spherules. Note protrusions on surface (scale bar 10 mm).

Fig 15. Thin section (plain polarized light) of Albion Formation diamictite bed altered glass shard (palagonite and smectite) showing relict vesicles with concentric alteration patterns (scale bar 0.5 mm).

Fig. 16. Albion Formation diamictite bed shocked quartz grain showing two sets of planar deformation features (scale bar 20 μm).

Table 1
Major oxide analyses from the Albion Formation diamictite bed and spheroid bed, and from the K/T boundary in Haiti.

	Spheroid* Palagonite n = 12	Diamictite* Palagonite n = 11	Spheroid‡ Bulk Sample n = 3	Haiti K/T* Palagonite n = 5
Na_2O	0.06±0.02	0.06±0.05	0.04±0.02	0.6±0.2
MgO	9.65±0.72	8.56±0.51	17.60±1.91	6.5±0.4
Al_2O_3	16.70±1.17	16.42±0.67	3.69±2.17	15.7±1.6
SiO_2	58.21±3.27	57.33±2.31	11.05±6.70	61.1±1.8
K_2O	0.36±0.07	2.00±1.06	0.13±0.14	0.2±0.1
CaO	0.13±0.22	0.13±0.04	24.33±4.35	0.7±0.1
TiO_2	0.65±1.13	0.93±0.78	0.17±0.09	0.5±0.2
MnO	0.02±0.01	0.01±0.01	<0.01	no data
FeO	3.43±0.50	6.02±2.09	1.53±0.49	7.6±1.0
L.O.I.			41.57±3.39	
Total	89.20±4.95	91.46±2.25	100.13±0.15	92.9±3.5

*Microprobe analyses of palagonite shards selected under SEM, error one standard deviation. Haiti K/T spherule analyses from [7].
‡XRF analyses of oven-dried samples. L.O.I. = loss on ignition.

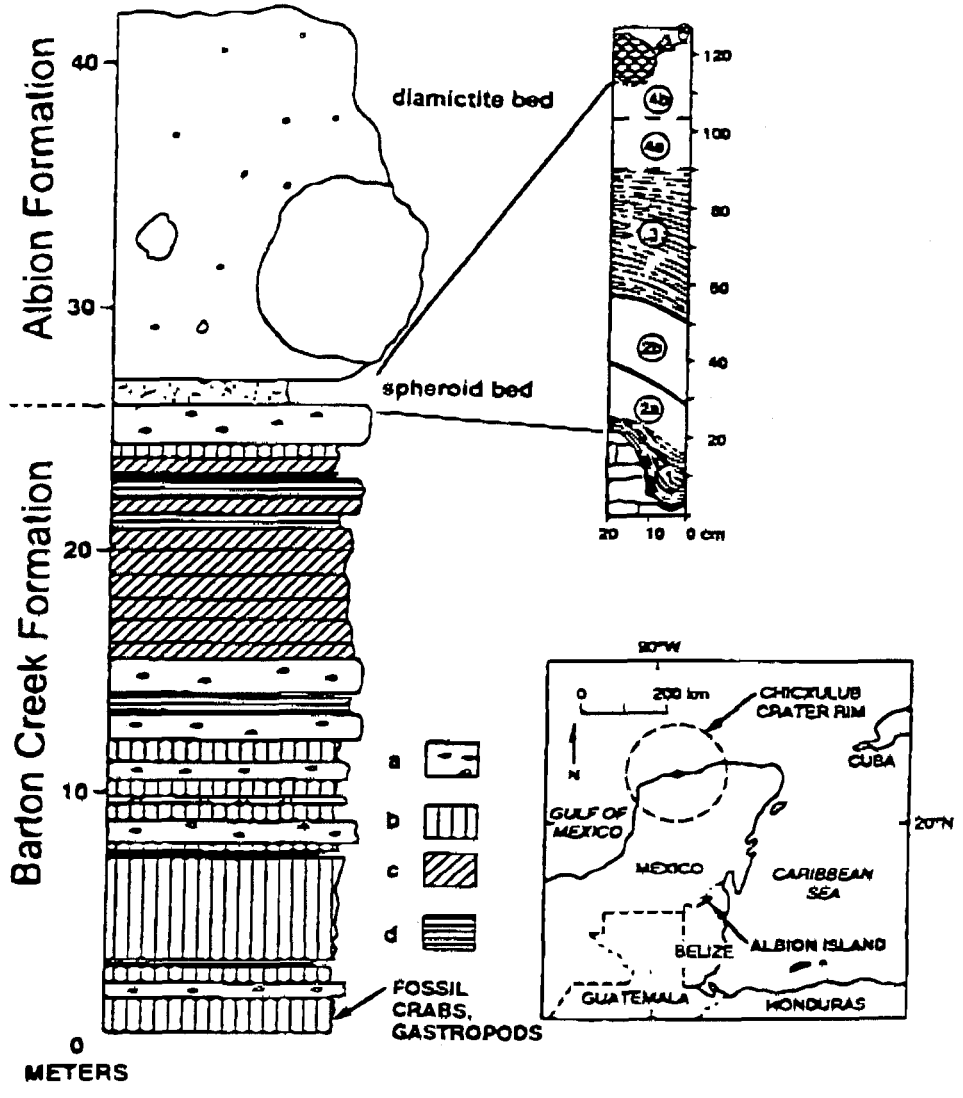

Fig. 1

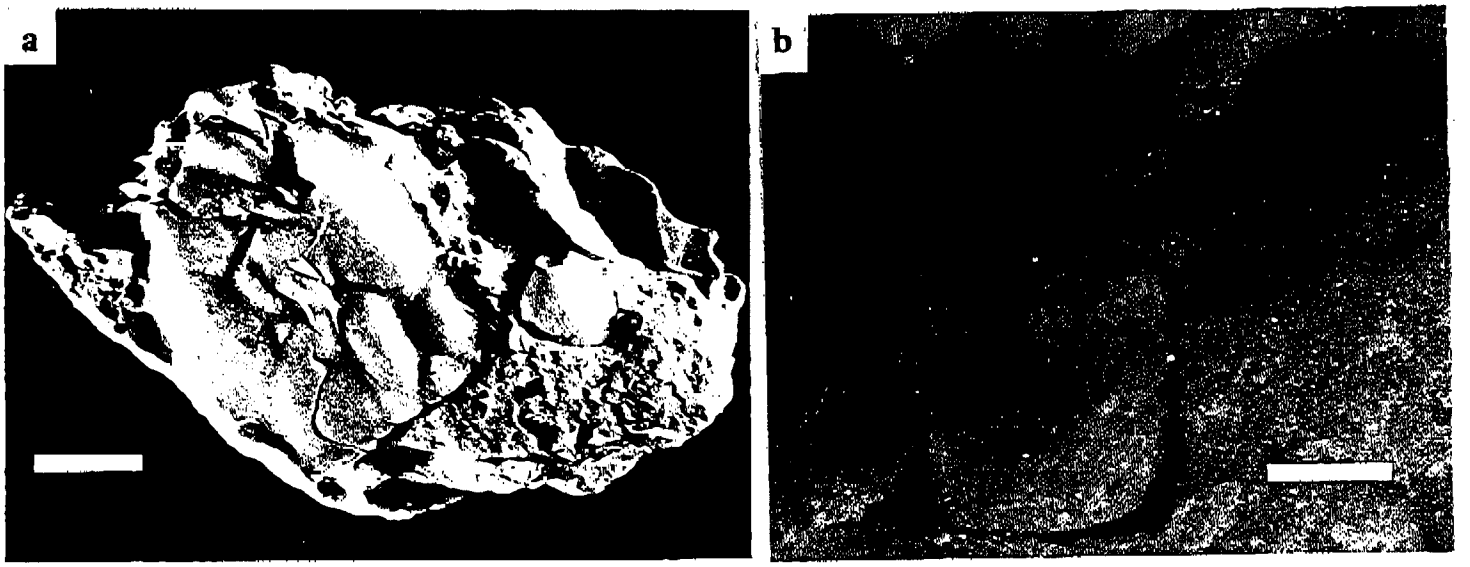

Fig. 2

Fig 3

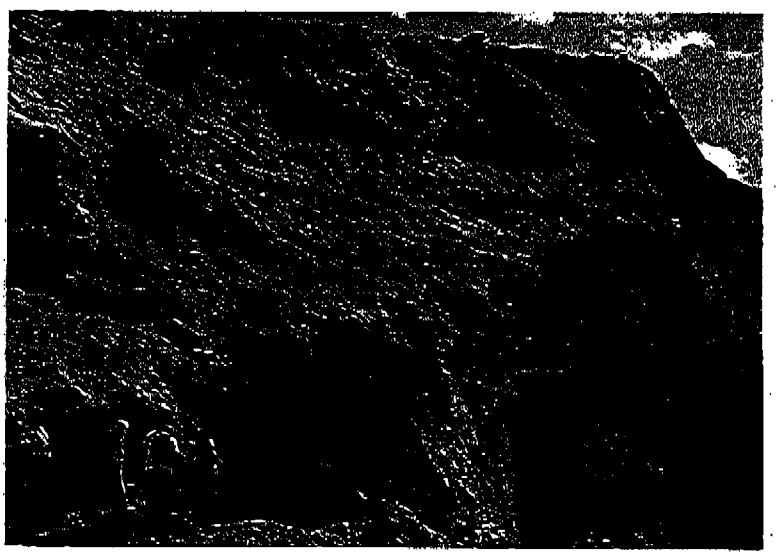

Fig. 4

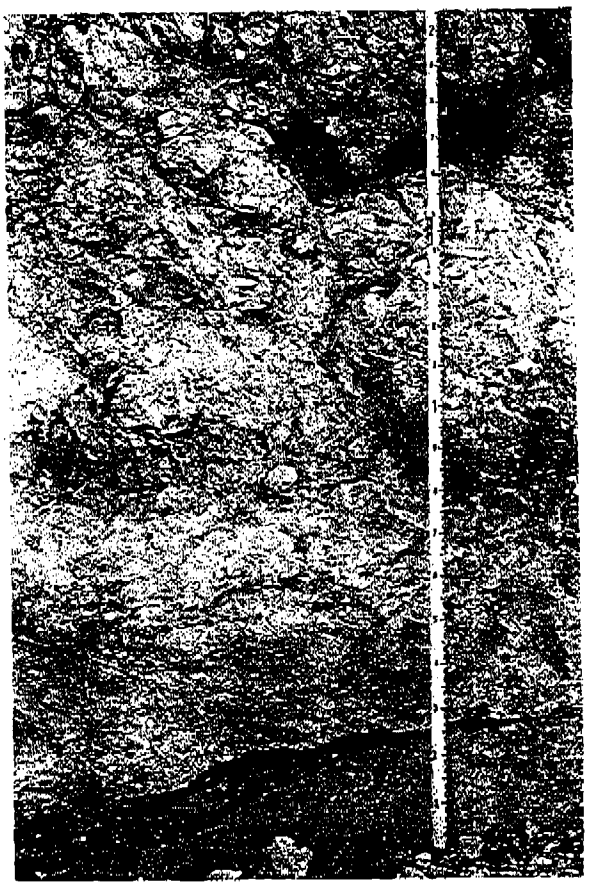

Fig. 5

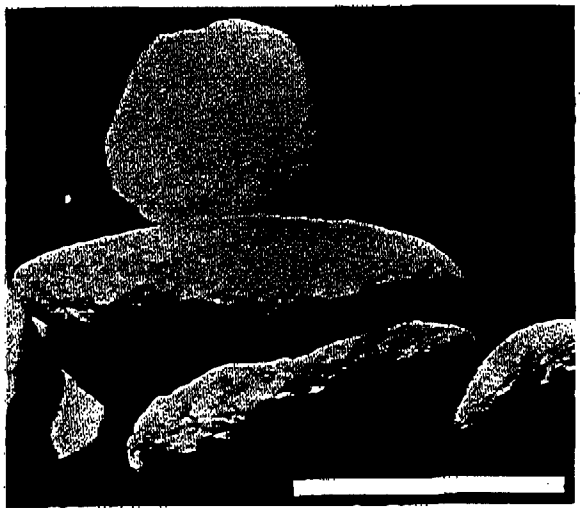

Fig. 6

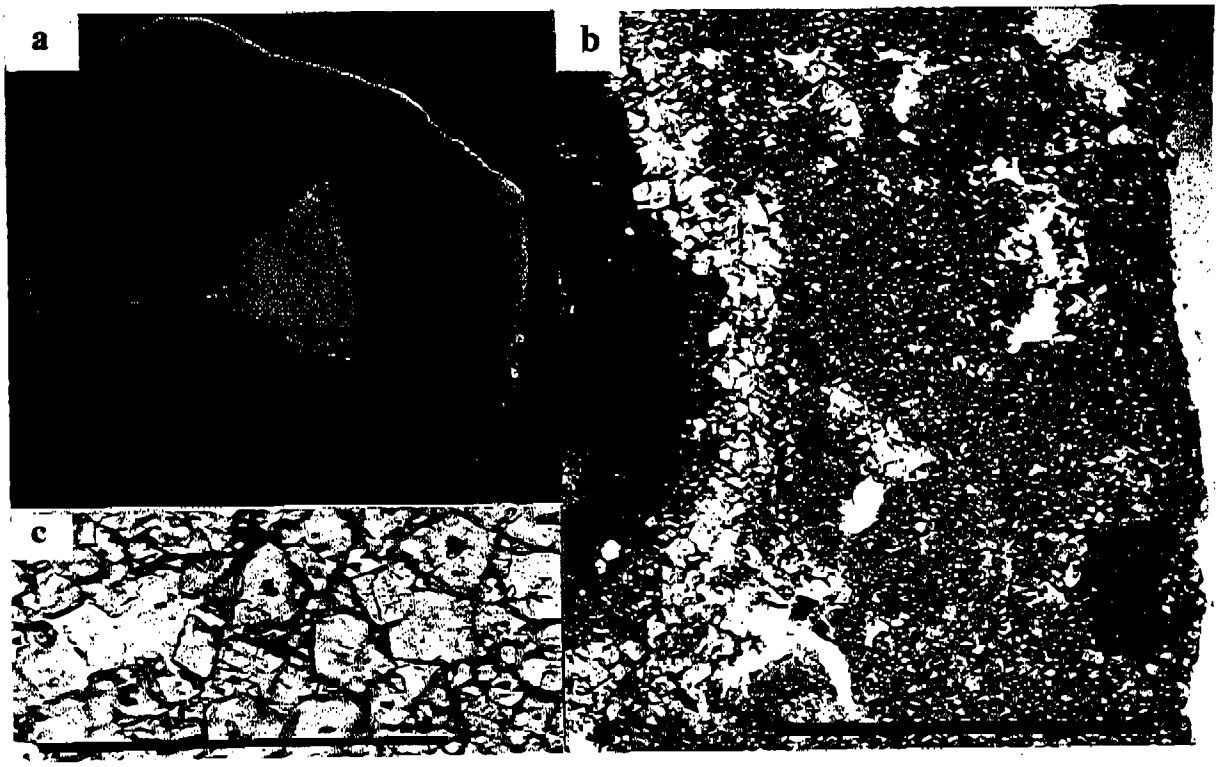

Fig. 7

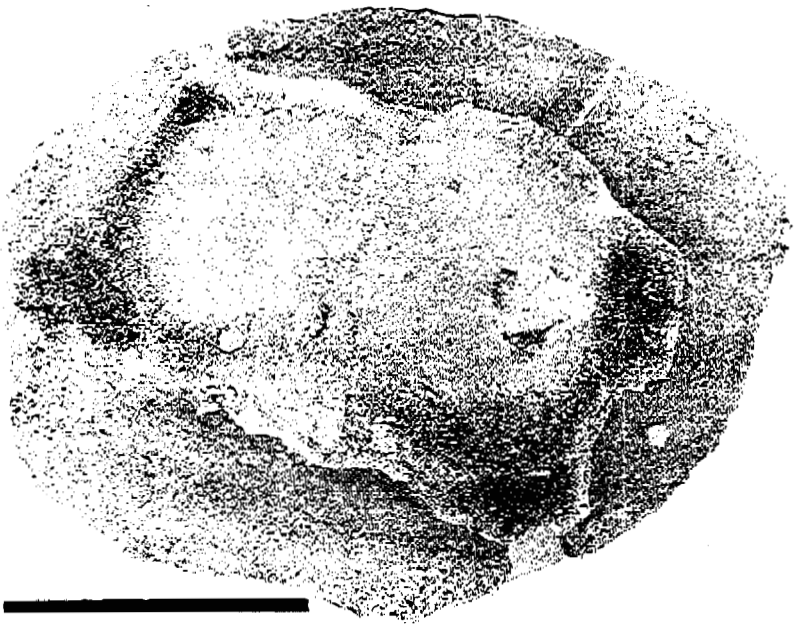

Fig. 8

Fig. 9

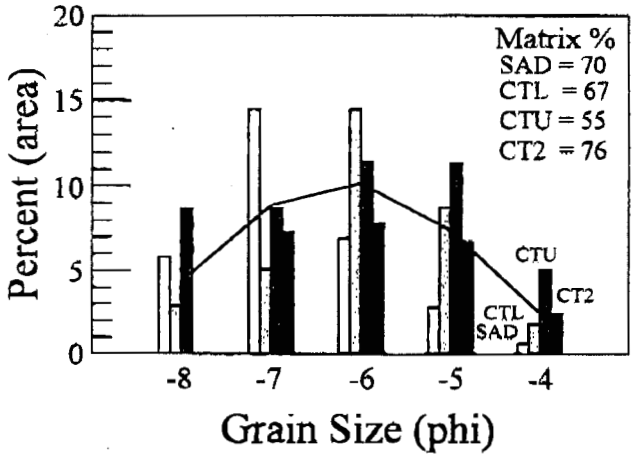

Fig. 10

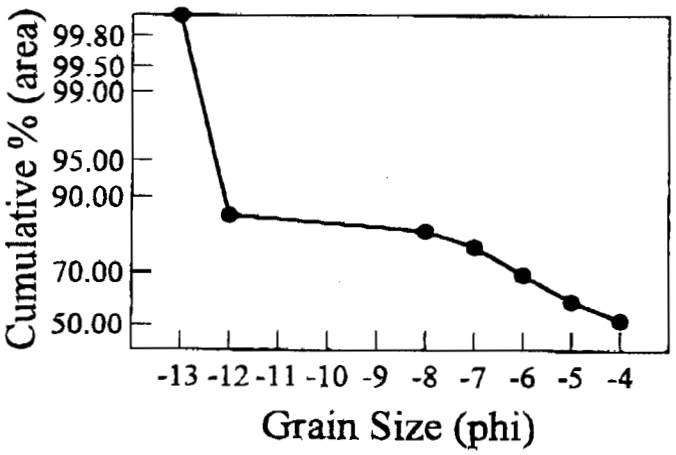

Fig. 11

Fig. 12

Fig. 13

Fig. 14

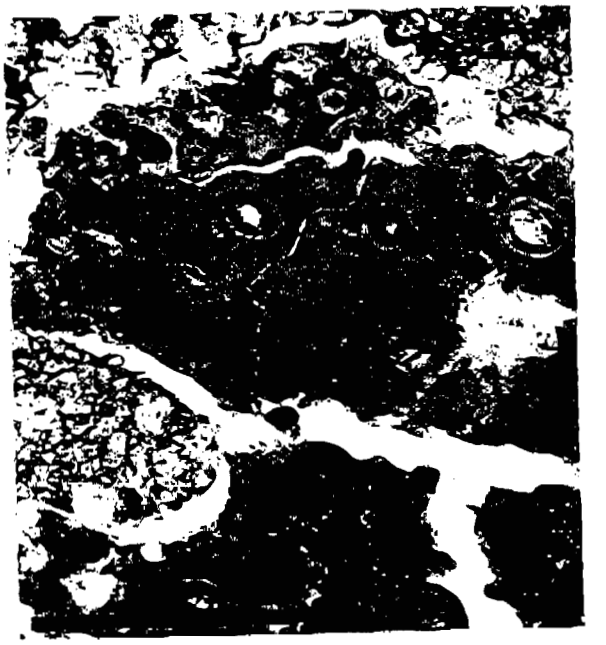

Fig. 15

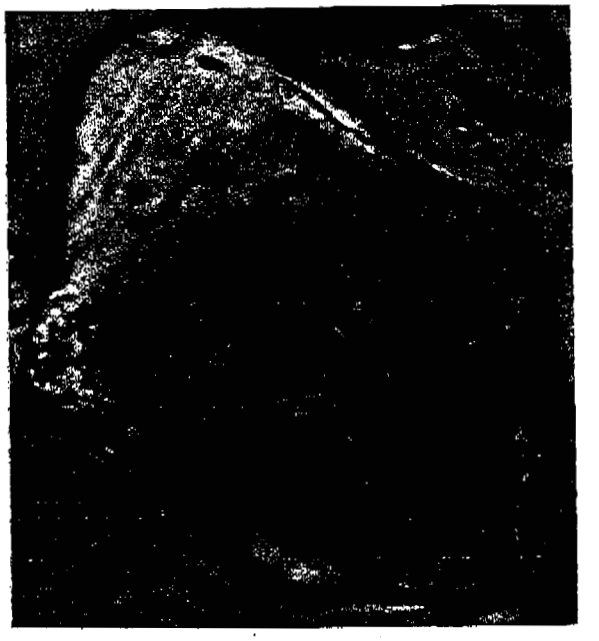

Fig. 16